Int. J. Solids Structures Vol. 27, No. 11, pp. 1461–1476, 1991
Printed in Great Britain.

0020–7683/91 $3.00 + .00

ROTATING ELASTIC–PLASTIC TUBE WITH FREE ENDS

WERNER MACK
Institut für Mechanik, Technische Universität Wien, Wiedner Hauptstraße 8–10, A-1040 Wien, Austria

(*Received* 24 *October* 1989; *in revised form* 5 *June* 1990)

Abstract—Based on Tresca's yield condition and the associated flow rule, the distribution of stress, strain and displacement in a rotating hollow cylinder of elastic–plastic material under generalized plane strain is discussed.

1. INTRODUCTION

Rotating tubes are found frequently in mechanical engineering. To better utilize the material, plastic deformation is admitted in many cases. However, most of the authors concerned with this topic [e.g. Davis and Connelly (1959), Rimrott (1960), Lenard and Haddow (1972), Lo and Abeyaratne (1981), Durban and Kubi (1990)] did not study partial yielding. The first analysis of a partially plastic, elastically compressible rotating tube is due to Gamer and Lance (1983), who assumed fixed ends.

The subject of this paper is the more intricate problem of a rotating elastic–perfectly plastic tube with free ends. The basis of this investigation is Tresca's yield condition and its associated flow rule. It is assumed that the tube retains its circular symmetry throughout the loading process and is sufficiently long for the stress and strain not to vary along the tube. Then, the principal directions of stress and strain are the radial, circumferential and axial directions.

In Fig. 1, Tresca's yield condition is represented in the usual way as a regular hexagon in the deviatoric plane of the three-dimensional principal stress space. This figure shows six phases of the development of plastic flow occurring in a rotating tube with inner boundary at $r = a$ and outer boundary at $r = b$. The denomination of the different elastic and plastic regions and the border radii separating them can be found in Fig. 2. At an angular speed $\omega = \omega_1$, plastic flow starts at the inner edge and spreads with increasing values of ω (Figs 1a and 1b). Next, for not too thin-walled tubes (see Section 3.3), the stress image point of the elastic–plastic border r_1 reaches at $\omega = \omega_2$ a corner of Tresca's hexagon and two additional plastic regions with different forms of the yield condition emerge (Figs 1c and 1d). Further increase in angular speed causes the stress image points of plastic region I to migrate into the corner and for $\omega \geqslant \omega_3$ two different plastic regions only remain inside the elastic outer shell (Fig. 1e). Finally, for $\omega = \omega_4$, the elastic region disappears and the tube attains a fully plastic state (Fig. 1f), which however is not its collapse state (see Section 4).

In Section 2, the basic equations of stresses and displacements in the elastic region and in the three different plastic regions will be determined by integration. In Section 3, the stress distributions in the tube are derived for different ranges of the load parameter. Finally, in Section 4, numerical results are presented and discussed.

2. BASIC EQUATIONS

2.1. *Elastic region*

The equation of equilibrium

$$\frac{\mathrm{d}\sigma_r}{\mathrm{d}r} + \frac{\sigma_r - \sigma_\theta}{r} = -\rho\omega^2 r, \tag{1}$$

and the geometric relations

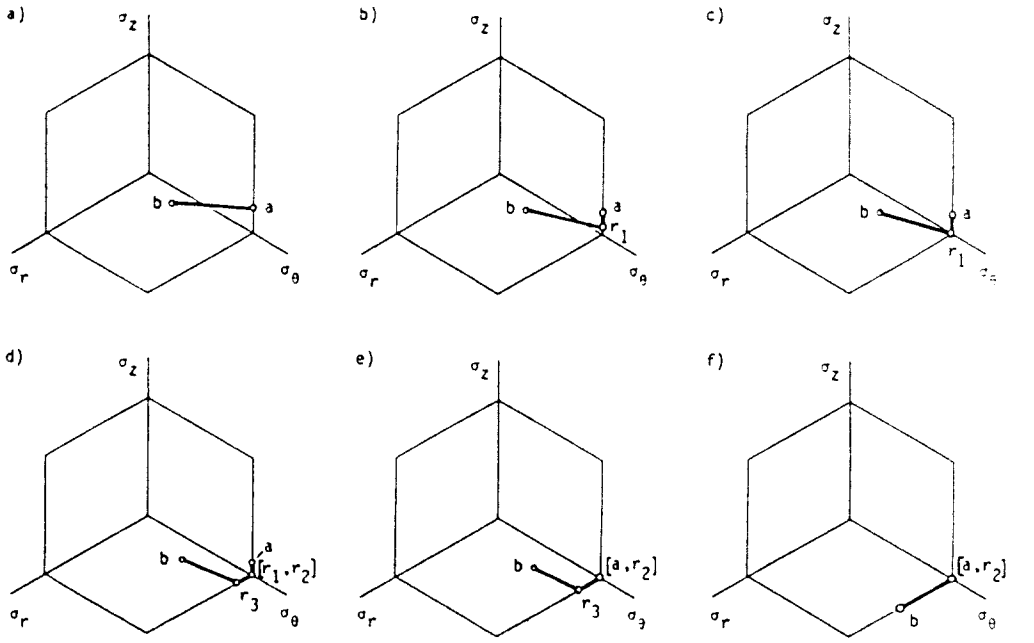

Fig. 1. Stress field in the rotating tube mapped onto the deviatoric plane of the principal stress space (sketch). (a) $\omega = \omega_1$, yielding starts at the inner boundary $r = a$; (b) $\omega_1 < \omega < \omega_2$, a plastic region spreads; (c) $\omega = \omega_2$, the axial stress equals the radial stress at the elastic-plastic border r_1; (d) $\omega_2 < \omega < \omega_3$, two additional plastic regions spread; (e) $\omega_3 \leqq \omega < \omega_4$, the first plastic region has disappeared; (f) $\omega = \omega_4$, the entire tube behaves plastically.

$$\varepsilon_r = \frac{\mathrm{d}u}{\mathrm{d}r}, \quad \varepsilon_\theta = \frac{u}{r} \tag{2}$$

hold in the entire tube, irrespective of the material behaviour.

In the elastic case, stresses and strains are related by Hooke's law

$$\sigma_r = 2G\left(\varepsilon_r + \frac{\nu}{1-2\nu}e\right), \quad \sigma_\theta = 2G\left(\varepsilon_\theta + \frac{\nu}{1-2\nu}e\right), \quad \sigma_z = 2G\left(\varepsilon_z + \frac{\nu}{1-2\nu}e\right), \tag{3}$$

where

$$e = \varepsilon_r + \varepsilon_\theta + \varepsilon_z \tag{4}$$

means the dilatation.

Considering (2)–(4) and the condition of generalized plane strain, $\varepsilon_z = \text{const}$, one obtains from the equation of equilibrium (1) a differential equation for the displacement

$$\frac{\mathrm{d}^2u}{\mathrm{d}r^2} + \frac{1}{r}\frac{\mathrm{d}u}{\mathrm{d}r} - \frac{u}{r^2} = -\frac{1-2\nu}{2(1-\nu)G}\rho\omega^2 r, \tag{5}$$

with the solution

$$u = \frac{C_1}{r} + C_2 r - \frac{1-2\nu}{16(1-\nu)G}\rho\omega^2 r^3. \tag{6}$$

The C_i indicate constants of integration. From (2)–(4) and (6), the stresses

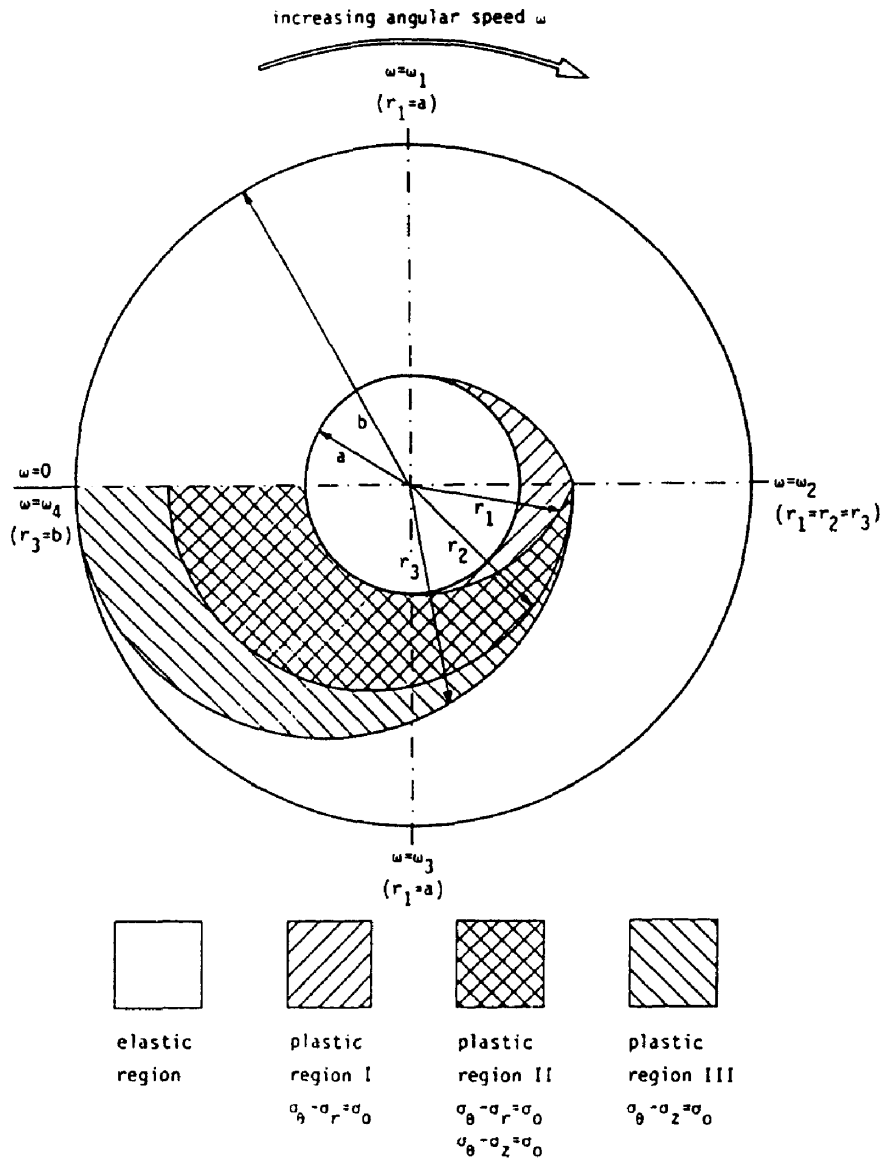

Fig. 2. Sketch of the elastic and plastic regions in the rotating tube.

$$\sigma_r = -2G\frac{C_1}{r^2} + \frac{2G}{1-2\nu}C_2 - \frac{3-2\nu}{8(1-\nu)}\rho\omega^2 r^2 + \frac{2\nu G}{1-2\nu}\varepsilon_z, \tag{7}$$

$$\sigma_\theta = 2G\frac{C_1}{r^2} + \frac{2G}{1-2\nu}C_2 - \frac{1+2\nu}{8(1-\nu)}\rho\omega^2 r^2 + \frac{2\nu G}{1-2\nu}\varepsilon_z, \tag{8}$$

$$\sigma_z = \nu(\sigma_r + \sigma_\theta) + 2(1+\nu)G\varepsilon_z \tag{9}$$

are arrived at.

2.2. *Plastic region I*, $\sigma_\theta > \sigma_z > \sigma_r$

Since σ_θ is the largest and σ_r the smallest stress, Tresca's yield condition adopts the form

$$\sigma_\theta - \sigma_r = \sigma_0, \tag{10}$$

where σ_0 denotes the uniaxial yield stress. Insertion of the yield condition into the equation of equilibrium (1) and integration gives

$$\sigma_r = \sigma_0 \ln r - \tfrac{1}{2}\rho\omega^2 r^2 + C_3, \tag{11}$$

$$\sigma_\theta = \sigma_0(1 + \ln r) - \tfrac{1}{2}\rho\omega^2 r^2 + C_3. \tag{12}$$

The flow rule leads to

$$\varepsilon_r^{\mathrm{pl}} = -\varepsilon_\theta^{\mathrm{pl}}, \quad \varepsilon_z^{\mathrm{pl}} = 0. \tag{13}$$

Therefore

$$\varepsilon_z = \varepsilon_z^{\mathrm{el}}, \tag{14}$$

and one obtains the same expression (9) for the axial stress as in the elastic case.

Because of plastic incompressibility, the dilatation is governed by Hooke's law,

$$e = \frac{1-2\nu}{2(1+\nu)G}(\sigma_r + \sigma_\theta + \sigma_z). \tag{15}$$

Thus, considering the geometric relations (2), a differential equation in u can be found,

$$\frac{\mathrm{d}u}{\mathrm{d}r} + \frac{u}{r} = \frac{1-2\nu}{2G}[\sigma_0(1 + 2\ln r) - \rho\omega^2 r^2 + 2C_3] - 2\nu\varepsilon_z. \tag{16}$$

Its solution is

$$u = \frac{1-2\nu}{2G}\left(\sigma_0 r \ln r - \tfrac{1}{4}\rho\omega^2 r^3 + C_3 r + \frac{C_4}{r}\right) - \nu\varepsilon_z r. \tag{17}$$

The difference between the total strain ε_θ and its elastic part $\varepsilon_\theta^{\mathrm{el}}$, which is calculated with the help of Hooke's law, gives the plastic strains

$$\varepsilon_\theta^{\mathrm{pl}} = -\varepsilon_r^{\mathrm{pl}} = \frac{1-2\nu}{2G}\left(\frac{1}{4}\rho\omega^2 r^2 + \frac{C_4}{r^2}\right) - \frac{1-\nu}{2G}\sigma_0. \tag{18}$$

2.3. *Plastic region II, $\sigma_\theta > \sigma_r = \sigma_z$*

In this plastic region, the stress state is in an "edge regime" of Tresca's prism with

$$\sigma_r = \sigma_z \tag{19}$$

and the yield condition reads

$$\sigma_\theta - \sigma_r = \sigma_0, \quad \sigma_\theta - \sigma_z = \sigma_0. \tag{20}$$

Integration of the equation of equilibrium (1) together with the yield condition leads to

$$\sigma_r = \sigma_z = \sigma_0 \ln r - \tfrac{1}{2}\rho\omega^2 r^2 + C_5, \tag{21}$$

$$\sigma_\theta = \sigma_0(1 + \ln r) - \tfrac{1}{2}\rho\omega^2 r^2 + C_5. \tag{22}$$

From the condition of plastic incompressibility (15), a differential equation in u can be derived,

$$\frac{du}{dr}+\frac{u}{r}=\frac{1-2\nu}{2(1+\nu)G}[\sigma_0(1+3\ln r)-\tfrac{3}{2}\rho\omega^2r^2+3C_5]-\varepsilon_z. \tag{23}$$

with the solution

$$u=\frac{1-2\nu}{4(1+\nu)G}[\sigma_0 r(-\tfrac{1}{2}+3\ln r)-\tfrac{3}{4}\rho\omega^2r^3+3C_5r]+\frac{C_6}{r}-\tfrac{1}{2}\varepsilon_z r. \tag{24}$$

Again, the plastic parts of the strains are found as the difference between the total strains and their elastic parts:

$$\varepsilon_r^{pl}=\frac{1-2\nu}{4(1+\nu)G}\left\{\sigma_0\left[\frac{5-6\nu}{2(1-2\nu)}+\ln r\right]-\tfrac{3}{4}\rho\omega^2r^2+C_5\right\}-\frac{C_6}{r^2}-\tfrac{1}{2}\varepsilon_z, \tag{25}$$

$$\varepsilon_\theta^{pl}=\frac{1-2\nu}{4(1+\nu)G}\left\{\sigma_0\left[-\frac{5-2\nu}{2(1-2\nu)}+\ln r\right]+\tfrac{1}{4}\rho\omega^2r^2+C_5\right\}+\frac{C_6}{r^2}-\tfrac{1}{2}\varepsilon_z, \tag{26}$$

$$\varepsilon_z^{pl}=\frac{1-2\nu}{4(1+\nu)G}\left[2\sigma_0\left(\frac{\nu}{1-2\nu}-\ln r\right)+\rho\omega^2r^2-2C_5\right]+\varepsilon_z. \tag{27}$$

2.4. *Plastic region III*, $\sigma_\theta > \sigma_r > \sigma_z$

Here, the yield condition adopts the form

$$\sigma_\theta-\sigma_z=\sigma_0. \tag{28}$$

As a consequence of the flow rule,

$$\varepsilon_\theta^{pl}=-\varepsilon_z^{pl},\quad \varepsilon_r^{pl}=0. \tag{29}$$

Hence

$$\varepsilon_r=\varepsilon_r^{el} \tag{30}$$

and

$$\varepsilon_\theta=\varepsilon_\theta^{el}+\varepsilon_\theta^{pl}=\varepsilon_\theta^{el}+\varepsilon_z^{el}-\varepsilon_z. \tag{31}$$

Next, these strains are inserted into the compatibility condition

$$\varepsilon_r=\frac{d}{dr}(\varepsilon_\theta r). \tag{32}$$

Their elastic parts can be expressed in terms of the stresses via Hooke's law, so that

$$\sigma_r-\nu(2\sigma_\theta-\sigma_0)=(1-\nu)\left[2\frac{d}{dr}(\sigma_\theta r)-\sigma_0\right]-2\nu\frac{d}{dr}(\sigma_r r)-2(1+\nu)G\varepsilon_z. \tag{33}$$

In this derivation, use has been made of the yield condition (28) and the condition of generalized plane strain, $\varepsilon_z=$ const. With the help of the equation of equilibrium (1), one obtains

$$r^2\frac{d^2\sigma_\theta}{dr^2}+3r\frac{d\sigma_\theta}{dr}+(1-R^2)\sigma_\theta=\frac{1-R^2}{1-2\nu}[\sigma_0-(1+6\nu)\rho\omega^2r^2+2(1+\nu)G\varepsilon_z] \tag{34}$$

where

$$R^2=\frac{1}{2(1-\nu)}. \tag{35}$$

The solution of (34) is

$$\sigma_\theta=C_7r^{-(1-R)}+C_8r^{-(1+R)}+\frac{1}{1-2\nu}\sigma_0-\frac{1+6\nu}{17-18\nu}\rho\omega^2r^2+\frac{2(1+\nu)G}{1-2\nu}\varepsilon_z. \tag{36}$$

From (1) there follows

$$\sigma_r=\frac{C_7}{R}r^{-(1-R)}-\frac{C_8}{R}r^{-(1+R)}+\frac{1}{1-2\nu}\sigma_0-\frac{2(3-2\nu)}{17-18\nu}\rho\omega^2r^2+\frac{2(1+\nu)G}{1-2\nu}\varepsilon_z \tag{37}$$

and from the yield condition (28)

$$\sigma_z=C_7r^{-(1-R)}+C_8r^{-(1+R)}+\frac{2\nu}{1-2\nu}\sigma_0-\frac{1+6\nu}{17-18\nu}\rho\omega^2r^2+\frac{2(1+\nu)G}{1-2\nu}\varepsilon_z. \tag{38}$$

Now, (31) and (36)–(38) yield the displacement

$$u=\frac{1}{(1+\nu)G}\left[\left(1-\nu-\frac{\nu}{R}\right)C_7r^R+\left(1-\nu+\frac{\nu}{R}\right)C_8r^{-R}\right]+\frac{1}{2G}\sigma_0r-\frac{1-2\nu}{(17-18\nu)G}\rho\omega^2r^3+\varepsilon_zr. \tag{39}$$

Finally, since $\varepsilon_\theta^{pl}=-\varepsilon_z^{pl}=\varepsilon_z^{el}-\varepsilon_z$, Hooke's law gives the plastic strains

$$\varepsilon_\theta^{pl}=-\varepsilon_z^{pl}=\frac{1}{2(1+\nu)G}\left[\left(1-\nu-\frac{\nu}{R}\right)C_7r^{-(1-R)}+\left(1-\nu+\frac{\nu}{R}\right)C_8r^{-(1+R)}-\frac{(1+\nu)(1-2\nu)}{17-18\nu}\rho\omega^2r^2\right]. \tag{40}$$

For $\varepsilon_z=0$, the basic equations of Gamer and Sayir (1984) for a plastic region of this type are recovered.

3. STRESS DISTRIBUTIONS IN THE TUBE

3.1. *In the elastic range $\omega\leqslant\omega_1$*

The equations for the displacement and the stresses contain the three unknowns C_1, C_2 and ε_z. In order to determine them, three conditions have to be found. Two of them read:

$$r=a:\quad \sigma_r=0, \tag{41}$$

$$r=b:\quad \sigma_r=0. \tag{42}$$

The third follows from the assumption of free ends, which implies that the total axial force on any section is equal to zero,

$$2\pi \int_a^b \sigma_z r \, dr = 0. \tag{43}$$

In Appendix A, a list of these integrals is given for the different elastic and plastic regions.

Making use of the above conditions, one ends up with

$$C_1 = \frac{3-2\nu}{16(1-\nu)G} \rho\omega^2 a^2 b^2, \tag{44}$$

$$C_2 = \frac{(1-2\nu)(3-2\nu)}{16(1-\nu)G} \rho\omega^2 (a^2+b^2) - \nu\varepsilon_z, \tag{45}$$

where

$$\varepsilon_z = \frac{-\nu}{4(1+\nu)G} \rho\omega^2 (a^2+b^2). \tag{46}$$

3.2. *In the elastic–plastic range* $\omega_1 \leqslant \omega \leqslant \omega_2$

Since in the elastic tube the difference between the circumferential and radial stress is independent of the axial strain, yielding starts at the same angular speed

$$\omega = \omega_1 = \sqrt{\frac{4(1-\nu)\sigma_0}{\rho[(1-2\nu)a^2+(3-2\nu)b^2]}} \tag{47}$$

as in the fixed end case (Gamer and Lance, 1983) at the inner boundary $r = a$. In the subsequent load range, the tube is composed of plastic region I and the outer elastic region. Besides the elastic–plastic interface radius r_1 there are five more unknowns: C_1, C_2, C_3, C_4 and ε_z. The conditions for their determination read (in the following, the superscript denotes the region):

$$r = a: \quad \sigma_r^{(I)} = 0, \tag{48}$$

$$r = r_1: \quad \sigma_r^{(I)} = \sigma_r^{(el)}, \tag{49}$$

$$u^{(I)} = u^{(el)}, \tag{50}$$

$$\sigma_\theta^{(el)} - \sigma_r^{(el)} = \sigma_0, \tag{51}$$

$$r = b: \quad \sigma_r^{(el)} = 0. \tag{52}$$

Of course, the free end condition (43) is needed here again and also in the following phases of plastic flow.

From this, one obtains (see the remark in Appendix B)

$$C_1 = \frac{1}{4G}\left(\sigma_0 r_1^2 - \frac{1-2\nu}{4(1-\nu)} \rho\omega^2 r_1^4\right), \tag{53}$$

$$C_2 = \frac{1-2\nu}{4b^2G}\left\{\sigma_0 r_1^2 + \frac{1}{4(1-\nu)} \rho\omega^2[-(1-2\nu)r_1^4 + (3-2\nu)b^4]\right\} - \nu\varepsilon_z, \tag{54}$$

$$C_3 = -\sigma_0 \ln a + \tfrac{1}{2}\rho\omega^2 a^2, \tag{55}$$

$$C_4 = \frac{1-\nu}{1-2\nu}\sigma_0 r_1^2 - \tfrac{1}{4}\rho\omega^2 r_1^4. \tag{56}$$

The value of r_1 comes from

$$\sigma_0\left(\frac{1}{2}+\ln\frac{r_1}{a}-\frac{r_1^2}{2b^2}\right)+\frac{1}{8(1-\nu)}\rho\omega^2\left[(1-2\nu)\left(\frac{r_1^4}{b^2}-2r_1^2\right)+4(1-\nu)a^2-(3-2\nu)b^2\right]=0 \tag{57}$$

and expression (46) for ε_z holds again (see Appendix C).

3.3. *In the elastic–plastic range* $\omega_2 \leqslant \omega \leqslant \omega_3$

For $\omega = \omega_2$, σ_r and σ_z become equal at the elastic–plastic border r_1. At this radius, two additional plastic regions emerge. However, this holds true only if the tube is not too thin-walled. For $\nu = 0.3$, for example, one finds $a/b < 0.8491$. In thinner tubes σ_r and σ_z become equal somewhere in plastic region I. This case is not treated here.

The angular speed ω_2 and the radius $r_1(\omega_2)$ are obtained with the help of (57) and the condition

$$\sigma_\theta^{(I)}(r_1(\omega_2),\omega_2)-\sigma_z^{(I)}(r_1(\omega_2),\omega_2)=\sigma_0. \tag{58}$$

In the load range $\omega_2 \leqslant \omega \leqslant \omega_3$, there are 12 unknowns: C_1, C_2, C_3, C_4, C_5, C_6, C_7, C_8, r_1, r_2, r_3 and ε_z. In order to determine them, the following conditions are available:

$$r = a: \quad \sigma_r^{(I)} = 0, \tag{59}$$

$$r = r_1: \quad \sigma_r^{(I)} = \sigma_r^{(II)}, \tag{60}$$

$$u^{(I)} = u^{(II)}, \tag{61}$$

$$\sigma_\theta^{(I)} - \sigma_z^{(I)} = \sigma_0, \tag{62}$$

$$r = r_2: \quad \sigma_r^{(II)} = \sigma_r^{(III)}, \tag{63}$$

$$u^{(II)} = u^{(III)}, \tag{64}$$

$$\sigma_\theta^{(III)} - \sigma_r^{(III)} = \sigma_0, \tag{65}$$

$$r = r_3: \quad \sigma_r^{(III)} = \sigma_r^{(el)}, \tag{66}$$

$$u^{(III)} = u^{(el)}, \tag{67}$$

$$\sigma_\theta^{(el)} - \sigma_z^{(el)} = \sigma_0, \tag{68}$$

$$r = b: \quad \sigma_r^{(el)} = 0. \tag{69}$$

They are completed by the free end condition (43).

Again, the constants of integration are expressed in terms of the radii r_1, r_2 and r_3. It is convenient to compute them—as far as possible—for the regions adjacent to the tube's boundaries first, and then for the central regions:

$$C_1 = \frac{r_3^2 b^2}{2[(1-2\nu)r_3^2 + b^2]G}\left\{\sigma_0 + \frac{1-2\nu}{8(1-\nu)}\rho\omega^2[r_3^2 - (3-2\nu)b^2] + 2(1+\nu)G\varepsilon_z\right\}, \quad (70)$$

$$C_2 = \frac{1-2\nu}{2[(1-2\nu)r_3^2 + b^2]G}\left\{\sigma_0 r_3^2 + \frac{1}{8(1-\nu)}\rho\omega^2[(1-2\nu)r_3^4 + (3-2\nu)b^4] + 2\left(r_3^2 - \frac{\nu}{1-2\nu}b^2\right)G\varepsilon_z\right\}, \quad (71)$$

$$C_3 = C_5 = -\sigma_0 \ln a + \tfrac{1}{2}\rho\omega^2 a^2, \quad (72)$$

$$C_7 = \frac{1-\nu+\dfrac{\nu}{R}}{2(1-\nu)} R r_3^{1-R}\left\{\frac{-1}{1-2\nu}\sigma_0 - (3-2\nu)\left[\frac{1}{8(1-\nu)} - \frac{2}{17-18\nu}\right]\rho\omega^2 r_3^2 - \frac{2}{1-2\nu}G\varepsilon_z - 2G\left(\frac{C_1}{r_3^2} - \frac{C_2}{1-2\nu}\right)\right\} + \frac{1+\nu}{2(1-\nu)} r_3^{1-R}\left\{-\tfrac{1}{2}\sigma_0 - \frac{1-2\nu}{2}\left[\frac{1}{8(1-\nu)} - \frac{2}{17-18\nu}\right]\rho\omega^2 r_3^2 - G\varepsilon_z + G\left(\frac{C_1}{r_3^2} + C_2\right)\right\}, \quad (73)$$

$$C_8 = R r_3^{1+R}\left\{\frac{C_7}{R} r_3^{(1-R)} + \frac{1}{1-2\nu}\sigma_0 + (3-2\nu)\left[\frac{1}{8(1-\nu)} - \frac{2}{17-18\nu}\right]\rho\omega^2 r_3^2 + \frac{2G}{1-2\nu}\varepsilon_z + 2G\left(\frac{C_1}{r_3^2} - \frac{C_2}{1-2\nu}\right)\right\}, \quad (74)$$

$$C_6 = \frac{1}{(1+\nu)G}\left[\left(1-\nu-\frac{\nu}{R}\right)C_7 r_2^{1+R} + \left(1-\nu+\frac{\nu}{R}\right)C_8 r_2^{1-R}\right] + \frac{r_2^2}{G}\left\{\frac{1-2\nu}{4(1+\nu)}\left[\sigma_0\left(\frac{1}{2} - 3\ln\frac{r_2}{a}\right) - \tfrac{3}{2}\rho\omega^2(a^2 - \tfrac{1}{3}r_2^2)\right] + \tfrac{1}{2}\sigma_0 - \frac{1-2\nu}{17-18\nu}\rho\omega^2 r_2^2 + \tfrac{1}{3}G\varepsilon_z\right\}, \quad (75)$$

$$C_4 = \frac{2G}{1-2\nu}C_6 + \frac{(1-2\nu)r_1^2}{2(1+\nu)}\left\{\sigma_0\left[\frac{-1}{2(1-2\nu)} + \ln\frac{r_1}{a}\right] + \tfrac{1}{2}\rho\omega^2(a^2 - \tfrac{1}{2}r_1^2)\right\} - G\varepsilon_z r_1^2. \quad (76)$$

The axial strain is given by

$$\varepsilon_z = \frac{-(1-2\nu)}{2(1+\nu)G}\left[\sigma_0\left(\frac{\nu}{1-2\nu} - \ln\frac{r_1}{a}\right) + \tfrac{1}{2}\rho\omega^2(r_1^2 - a^2)\right]. \quad (77)$$

In the derivation of these results, no use has been made of conditions (43), (63) and (65). They form a system of three equations in the three unknowns r_1, r_2 and r_3, which has to be solved numerically.

3.4. *In the elastic–plastic range* $\omega_3 \leqslant \omega \leqslant \omega_4$

With increasing angular speed, the interface r_1 between plastic regions I and II migrates to the inner boundary of the tube and reaches it when $\omega = \omega_3$. Hence, ω_3 can be found from the condition

$$r_1(\omega_3) = a. \quad (78)$$

In the subsequent load range, plastic region I vanishes and the unknowns r_1, C_3 and C_4

drop. There remain the nine unknowns C_1, C_2, C_5, C_6, C_7, C_8, r_2, r_3 and ε_z. In order to determine them, conditions (43) and (63)–(69) are still valid. They are completed by

$$r = a: \quad \sigma_r^{(II)} = 0. \tag{79}$$

While the results for the constants of integration are retained without change, eqns (43), (63) and (65) are used here to calculate r_2, r_3 and ε_z. Although this system of three equations could be reduced by one using a lengthy expression for $\varepsilon_z(r_2, r_3)$, it is more convenient to solve the whole system numerically.

3.5. *In the totally plastic range* $\omega_4 \leqslant \omega\ (\leqslant \omega_5)$

At $\omega = \omega_4$, the elastic region disappears and the entire tube is plasticized. Thus, the angular speed ω_4 is found from the condition

$$r_3(\omega_4) = b. \tag{80}$$

Since a further small increase in angular speed beyond ω_4 is possible (see Section 4), the constants of integration and the equations for r_2 and ε_z in the following load range are given. Making use of conditions (43), (63)–(65), (79) and

$$r = b: \quad \sigma_r^{(III)} = 0, \tag{81}$$

one derives

$$C_7 = \frac{-(1+R)b^{1+R}r_2^{(1+R)}\left[\dfrac{1}{1-2\nu}\sigma_0 - \dfrac{2(3-2\nu)}{17-18\nu}\rho\omega^2b^2 + \dfrac{2(1+\nu)G}{1-2\nu}\varepsilon_z\right] + \sigma_0 - \dfrac{5(1-2\nu)}{17-18\nu}\rho\omega^2r_2^2}{\left(1-\dfrac{1}{R}\right)r_2^{(1-R)} + \left(1+\dfrac{1}{R}\right)b^{2R}r_2^{-(1+R)}}, \tag{82}$$

$$C_8 = Rb^{1+R}\left[\frac{C_7}{R}b^{-(1-R)} + \frac{1}{1-2\nu}\sigma_0 - \frac{2(3-2\nu)}{17-18\nu}\rho\omega^2b^2 + \frac{2(1+\nu)G}{1-2\nu}\varepsilon_z\right]. \tag{83}$$

C_5 and C_6 are calculated by means of (72) and (75), respectively. The interface r_2 and the axial strain ε_z (which could be expressed in terms of r_2 in principle) are determined with the help of (43) and (63).

The range of validity of the above equations has an upper limit $\omega = \omega_5$, for which the circumferential stress at the tube's outer boundary vanishes. However, a detailed investigation of the behaviour at such high rotational speeds is not meaningful within a geometrically linear theory.

4. NUMERICAL RESULTS

For the numerical treatment of the problem it is convenient to introduce the following non-dimensional quantities:

$$Q = a/b, \quad \tilde{u} = uE/(b\sigma_0), \quad x = r/b, \quad \tilde{\varepsilon}_i = \varepsilon_i E/\sigma_0, \quad \tilde{\sigma}_i = \sigma_i/\sigma_0, \quad \Omega = \rho\omega^2b^2/\sigma_0. \tag{84}$$

The stress distribution is discussed for $Q = 0.5$ and Poisson's number $\nu = 0.3$.

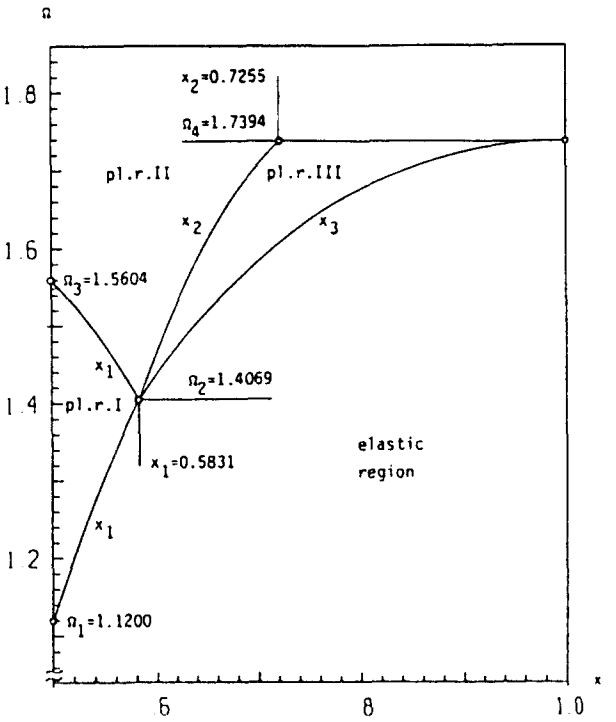

Fig. 3. Evolution of plastic regions with increasing angular speed.

First, Fig. 3 shows the evolution of the border radii with increasing Ω in the range $\Omega_1 \leqslant \Omega \leqslant \Omega_4$.

Figure 4 exhibits the stress distribution in the elastic tube just at the onset of plastic flow, and during the first elastic–plastic phase according to Sections 3.1 and 3.2, respectively. Note that for Ω_2 the radial stress equals the axial stress at the elastic–plastic border! Thereafter, two additional plastic regions emerge. The stresses in the subsequent flow phases, according to Sections 3.3–3.5, are depicted in Fig. 5. One should watch simultaneously the evolution of plastic deformation also on the deviatoric plane (Fig. 1) and on Fig. 6! Of course, the absolute value of the plastic strains presented in Fig. 6 grows monotonically with increasing angular speed.

Finally, Fig. 7 shows the displacements in the tube for four different angular speeds.

A point that has still to be discussed is the plastic collapse speed. As already mentioned in the Introduction, the angular speed Ω_4 corresponding to the totally plastic state is nevertheless not the plastic collapse speed. Indeed, the stress image point of the tube's outer boundary travels with increasing load towards the lower corner of Tresca's hexagon (see Fig. 1f), and reaches it for $\Omega_5 = 1.7500$. Then, a further increase in speed causes the formation and extension of a second plastic "edge regime" region and one can imagine that in the final state the tube would be composed of this new plastic region and the inner plastic region II, with an infinitely small plastic region III in between. The same stress distribution was obtained by Lenard and Haddow (1972) in their analysis of the plastic collapse speed. Figure 8 exhibits Ω_4 and the plastic collapse speed Ω_{pc} as functions of the ratio Q in the range $0.3 < Q < 0.82$. While the difference is negligible for thin-walled tubes, it becomes noticeable with decreasing values of Q.

Of particular interest are also the stresses remaining after the stand-still. As soon as the angular speed decreases, the whole tube behaves elastically again. Thus, the stresses in the completely unloaded state can be found by subtraction of the stresses occurring in an unlimited elastic tube from those in the actual tube at the same maximum angular speed Ω_m, provided that the residual stresses do not reach the yield limit. Indeed, secondary plastic flow can occur only in very thick-walled tubes (Mack, 1991).

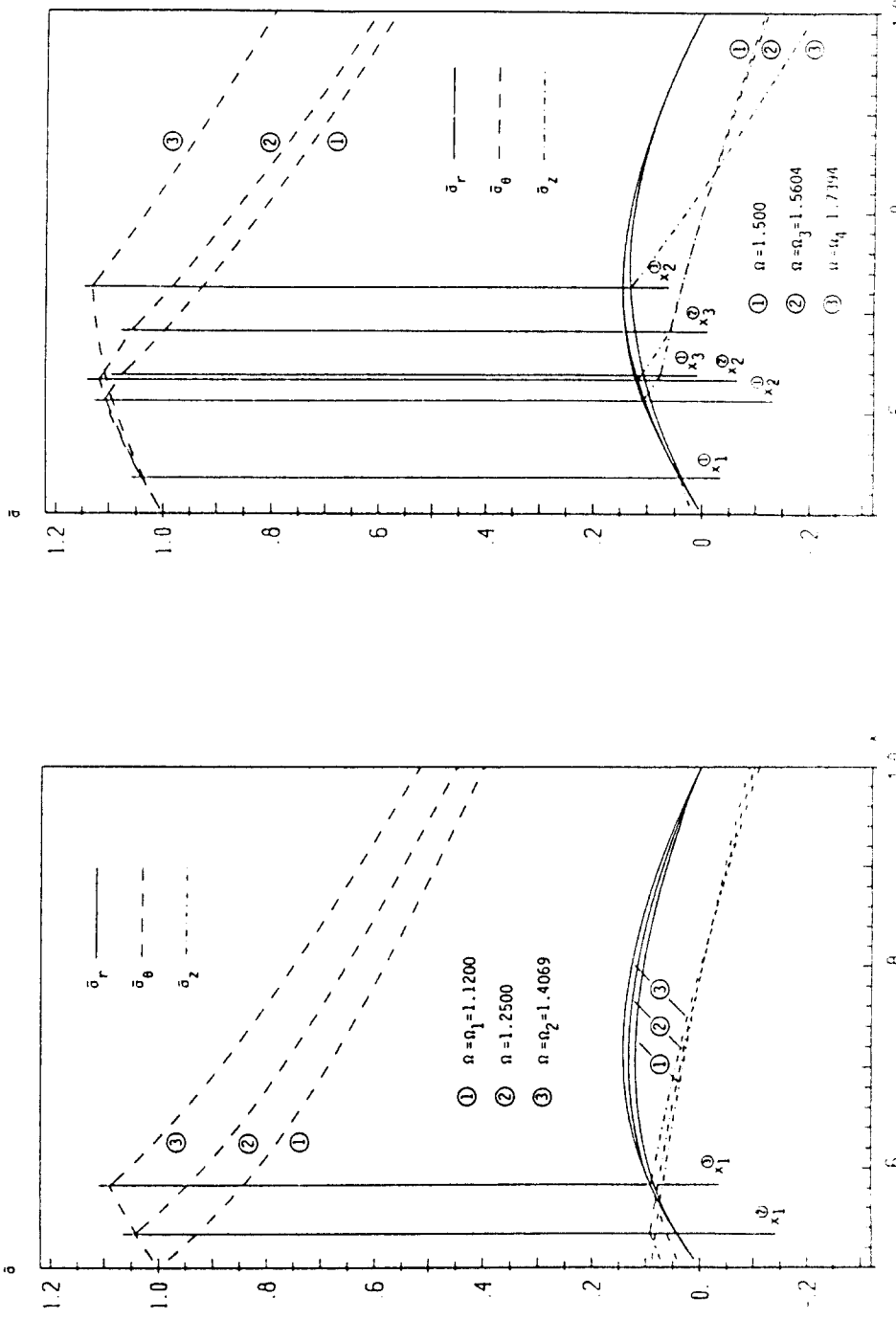

Fig. 4. Stresses during the elastic and the first elastic–plastic phase

Fig. 5. Stresses during the second and third elastic–plastic phase and in the totally plastic state.

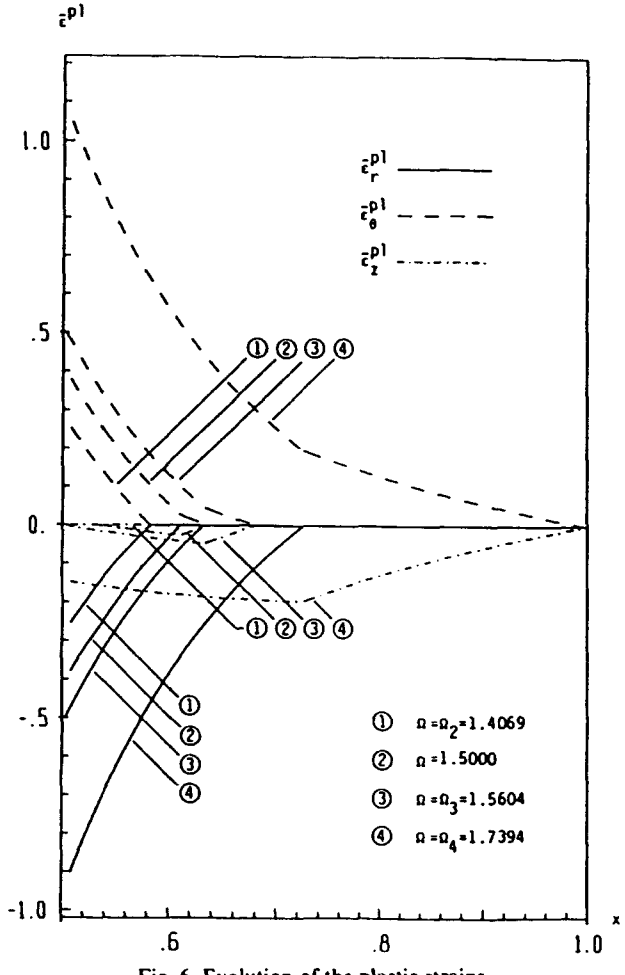

Fig. 6. Evolution of the plastic strains.

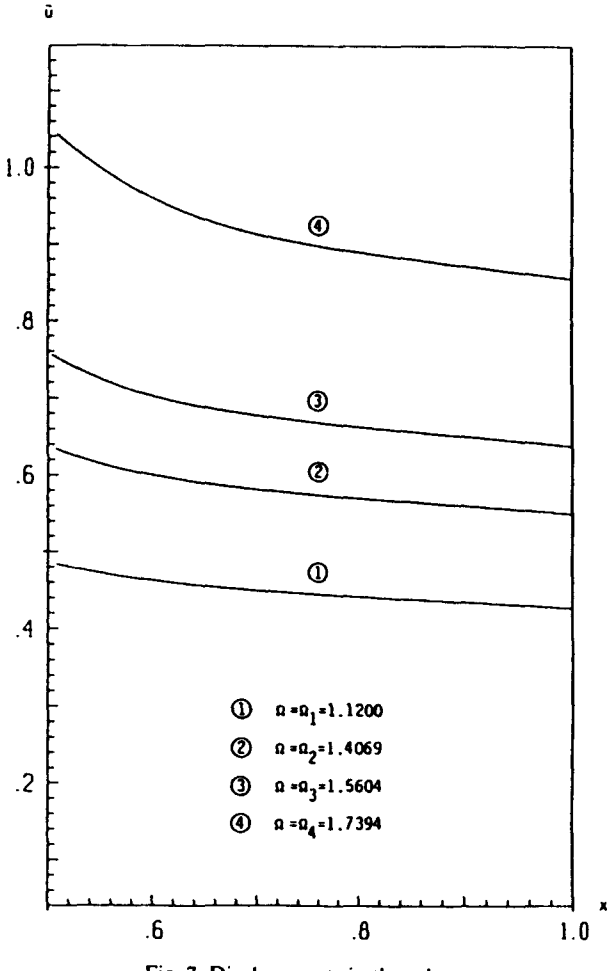

Fig. 7. Displacements in the tube.

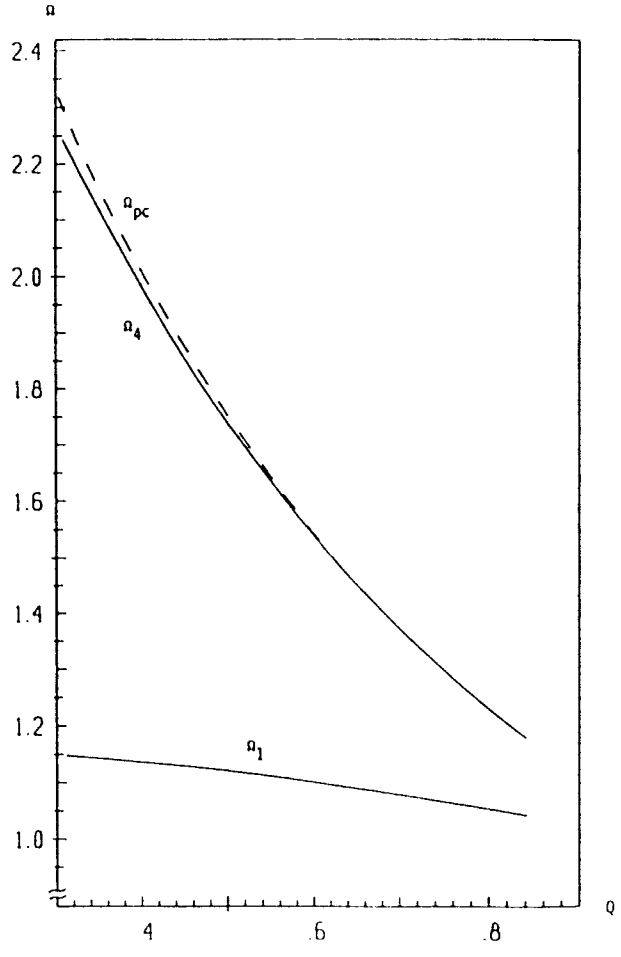

Fig. 8. Dependence of Ω_1, Ω_4 and Ω_{pc} (after Lenard and Haddow, 1972) on Q ($\nu = 0.3$).

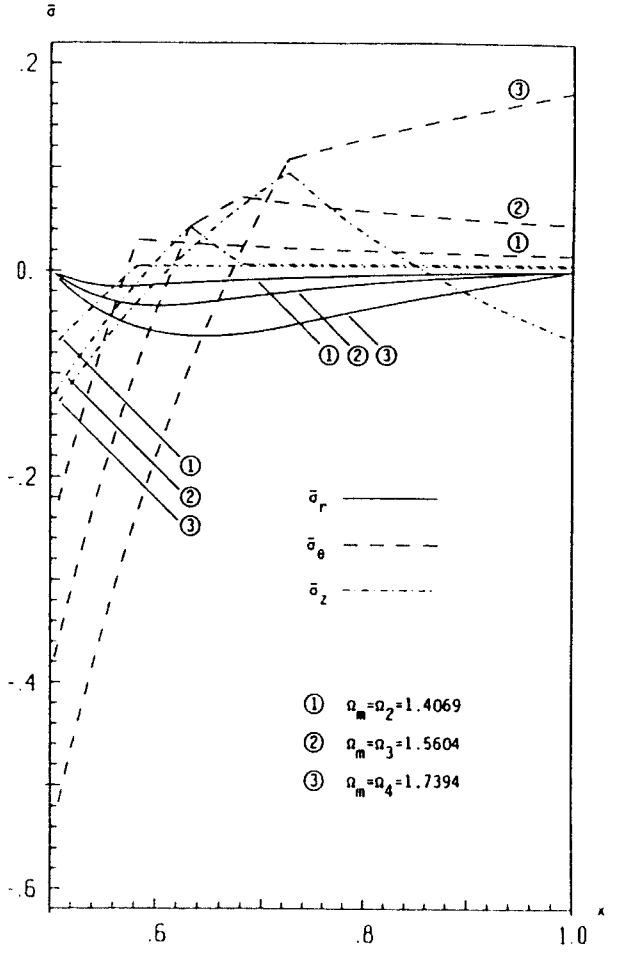

Fig. 9. Residual stresses for three different maximum angular speeds Ω_m.

Figure 9 shows the residual stresses in the tube with $Q = 0.5$ for three different maximum angular speeds. While the stresses in the radial and axial direction are comparatively small, the circumferential stress attains a significant extremum at the tube's inner boundary.

Acknowledgements—The author is indebted to Prof. Dr Udo Gamer for many helpful discussions and to the reviewer for the design of Fig. 2 and his valuable remarks.

REFERENCES

Bland, D. R. (1956). Elastoplastic thick-walled tubes of work-hardening material subject to internal and external pressures and to temperature gradients. *J. Mech. Phys. Solids* **4**, 209–229.

Davis, E. A. and Connelly, F. M. (1959). Stress distribution and plastic deformation in rotating cylinders of strain-hardening material. *J. Appl. Mech.* **26**, 25–30.

Durban, D. and Kubi, M. (1990). Large strain analysis for plastic-orthotropic tubes. *Int. J. Solids Structures* **26**, 483–495.

Gamer, U. and Lance, R. H. (1983). Stress distribution in a rotating elastic–plastic tube. *Acta Mech.* **50**, 1–8.

Gamer, U. and Sayir, M. (1984). Elastic–plastic stress distribution in a rotating solid shaft. *J. Appl. Math. Phys.* **35**, 601–617.

Lenard, J. and Haddow, J. B. (1972). Plastic collapse speeds for rotating cylinders. *Int. J. Mech. Sci.* **14**, 285–292.

Lo, K. K. and Abeyaratne, R. (1981). Finite elastic–plastic deformation of a rotating hollow cylinder. *J. Appl. Mech.* **48**, 666–668.

Mack, W. (1991). Entlastung und sekundäres Fließen in rotierenden elastisch–plastischen Hohlzylindern. *Z. Angew. Math. Mech.* (in press).

Rimrott, F. P. J. (1960). On the plastic behavior of rotating cylinders. *J. Appl. Mech.* **27**, 309–315.

APPENDIX A

The integrals

$$I(s,t) = \int_s^t \sigma_r r \, dr, \tag{A1}$$

where s and t denote two arbitrary radii, take the following forms:

(a) in the elastic region

$$I(s,t) = -\frac{\nu}{8(1-\nu)}\rho\omega^2(t^4-s^4) + \frac{G}{1-2\nu}[2\nu C_2 + (1-\nu)\varepsilon_z](t^2-s^2) \tag{A2}$$

(b) in plastic region I

$$I(s,t) = \nu\sigma_0(t^2\ln t - s^2\ln s) - \frac{\nu}{4}\rho\omega^2(t^4-s^4) + [\nu C_3 + (1+\nu)G\varepsilon_z](t^2-s^2) \tag{A3}$$

(c) in plastic region II

$$I(s,t) = \tfrac{1}{2}\sigma_0(t^2\ln t - s^2\ln s) + (\tfrac{1}{2}C_5 - \tfrac{1}{4}\sigma_0)(t^2-s^2) - \tfrac{1}{8}\rho\omega^2(t^4-s^4) \tag{A4}$$

(d) in plastic region III

$$I(s,t) = \frac{C_7}{1+R}(t^{1+R}-s^{1+R}) + \frac{C_8}{1-R}(t^{1-R}-s^{1-R}) + \frac{\nu}{1-2\nu}\sigma_0(t^2-s^2) - \frac{1+6\nu}{4(17-18\nu)}\rho\omega^2(t^4-s^4) + \frac{(1+\nu)G}{1-2\nu}\varepsilon_z(t^2-s^2). \tag{A5}$$

APPENDIX B

For $\omega > \omega_1$ one has to find the constants of integration, the axial strain, and the border radii separating the different elastic and plastic regions. The system of equations for their determination is non-linear in the border radii and linear in the other unknowns. To reduce the number of equations, the constants of integration and the axial strain can be expressed (in different forms) in terms of the border radii. The remaining non-linear equations then have to be solved numerically.

APPENDIX C

In the load range $\omega \leqslant \omega_2$ the axial strain can be derived in a way proposed by Bland (1956), too. Since $\varepsilon_z = \varepsilon_z^{el}$ both in the elastic region and in plastic region I, relation (9) for the axial stress holds throughout the tube. With the help of the equation of equilibrium (1), one can express σ_z in terms of σ_r,

$$\sigma_z = \nu\left(r\frac{d\sigma_r}{dr} + 2\sigma_r + \rho\omega^2 r^2\right) + 2(1+\nu)G\varepsilon_z. \tag{C1}$$

Insertion of this expression into the free end condition (43) and integration yields

$$\nu[b^2\sigma_r(b) - a^2\sigma_r(a) + \tfrac{1}{4}\rho\omega^2(b^4 - a^4)] + (1+\nu)G\varepsilon_z(b^2 - a^2) = 0. \tag{C2}$$

From this, using the conditions $\sigma_r(a) = \sigma_r(b) = 0$, one obtains

$$\varepsilon_z = \frac{-\nu}{4(1+\nu)G}\rho\omega^2(a^2 + b^2). \tag{C3}$$